Global Circulation in an Axially Symmetric Shallow-Water Model, Forced by Off-Equatorial Differential Heating

ORI ADAM AND NATHAN PALDOR

The Fredy & Nadine Herrmann Institute of Earth Sciences, The Hebrew University of Jerusalem, Jerusalem, Israel

ABSTRACT

An axially symmetric inviscid shallow-water model (SWM) on the rotating Earth forced by off-equatorial steady differential heating is employed to characterize the main features of the upper branch of an ideal Hadley circulation. The steady-state solutions are derived and analyzed and their relevance to asymptotic temporal evolution of the circulation is established by comparing them to numerically derived time-dependent solutions at long times. The main novel feature of the steady-state solutions of the present theory is the existence of a tropical region, associated with the rising branch of the Hadley circulation, which extends to about half the combined width of the Hadley cells in the two hemispheres and is dominated by strong vertical advection of momentum. The solutions in this tropical region are characterized by three conditions: (i) the meridional temperature gradient is very weak but drastically increases outside of the region, (ii) moderate easterlies exist only inside this region and they peak off the equator, and (iii) angular momentum is not conserved there. The momentum fluxes of the new solutions at the tropics differ qualitatively from those of existing nearly inviscid theories and the new flux estimates are in better agreement with both observations and axially symmetric simulations. As in previous nearly inviscid theories, the steady solutions of the new theory are determined by a thermal Rossby number and by the latitude of maximal heating.

---

1. Introduction

Axially symmetric models of the atmosphere describe the zonally averaged general circulation when large-scale eddies are suppressed. The contribution of macroturbulent and moist processes to the general circulation is best understood in comparison with inviscid, dry, axially symmetric mean states because the latter are special cases of the former. Therefore, even though outside the tropics solutions of axially symmetric models have limited applicability to the observed atmosphere, such models are of prime importance in elucidating the relative role of various processes. A review of the axially symmetric approach can be found in Schneider (2006).

Schneider and Lindzen (1977) and Schneider (1977) have shown that contrary to linear theories (e.g., Dickinson 1971), it is possible to maintain Hadley circulations even with small viscosities if nonlinear terms are not neglected.

Following Schneider (1977), Held and Hou (1980, hereafter HH80) have approximated the Hadley circulation in the nonlinear inviscid limit by using a simple set of assumptions: the zonal velocity at the ground is negligible with respect to the balanced wind at the upper branch, the upper branch conserves angular momentum, and the cell is energetically closed. The heating used as forcing in HH80 is Newtonian relaxation toward radiative equilibrium centered on the equator (equinoctial). The steady global circulation hypothesized by HH80 therefore follows a simple two-region paradigm: a tropical region where angular momentum is uniform, and extratropical regions where radiative equilibrium prevails. The angular momentum–conserving solutions (hereafter the AMC solutions) of HH80 have been generalized to off-equatorial heating distributions by Lindzen and Hou (1988, hereafter LH88).

The simplified AMC solutions of HH80 and LH88 as well as their many extensions (Hou 1984; Schneider 1987; Hou and Lindzen 1992; Plumb and Hou 1992; Fang and Tung 1996, 1997, 1999; and Polvani and Sobel 2002, to name a few) assume that the circulation is thermally driven and that (aside from friction) no sources of momentum exist, so that in general the absolute angular

Corresponding author address: Nathan Paldor, The Fredy & Nadine Herrmann Institute of Earth Sciences, The Hebrew University, Edmond J. Safra Campus, Givat Ram, Jerusalem 91904, Israel.
E-mail: nathan.paldor@huji.ac.il

momentum is materially conserved in the inviscid limit. In recent works, Walker and Schneider (2005, 2006) have shown that the abovementioned axially symmetric theories are not successful in predicting the extent and strength of the observed and simulated zonally averaged Hadley circulation, and that these theories yield erroneous momentum fluxes in the upper branches of the circulation. The momentum fluxes in any axially symmetric model (regardless of its additional assumptions) can be expected to differ from those of the zonally averaged atmosphere, since these models do not include momentum sources associated with macroturbulence. In addition to this inherent difference between axially symmetric models and the observed atmosphere, the AMC solutions (of HH80 and LH88) yield erroneous momentum fluxes (namely, the conservation of angular momentum) in the upper branches of the circulation even when compared with two-dimensional axially *symmetric* (i.e., eddy-free) simulations (Schneider 2006; see HH80's Fig. 6). These erroneous predictions are due to the neglect of vertical mixing of momentum at the rising branch of the circulation, as was suggested by HH80, Schneider (1987), LH88, and Walker and Schneider (2005), and are rectified by incorporating a region of strong mixing into the solutions, as was shown by Adam and Paldor (2009, hereafter AP09).

Shallow-water models (SWMs) that incorporate vertical advection of momentum have been used by Esler et al. (2000) and Shell and Held (2004). In these models, the flux of angular momentum into the Hadley cell originates from a stationary bottom layer that acts as a mass source for the upper layer. A discussion of the effect of the mass–momentum coupling in the SWM is given in AP09. AP09 also provided steady solutions of an axially symmetric SWM that accurately predict the momentum fluxes of the tropical upper branches of the axially symmetric circulation, for equinoctial heating. The AP09 theory differs from that of HH80 in that at the region of strong mixing, bottom and upper branch winds are homogenized, thus relaxing the unphysical HH80 assumption of negligibly small bottom winds in that region. In addition, AP09 differentiate the mixing region from the angular momentum–conserving region, thus providing solutions that follow a three-region paradigm instead of the two-region paradigm offered by HH80. While the existence of a strong mixing region was recognized by HH80 and LH88, both of these studies (as well as their numerous subsequent extensions) did not incorporate this region into their simplified analytic solutions, even though the width of the rising branch of the Hadley circulation in their numerical solutions extends to about half the width of the circulation cell.

The aim of this work is to extend AP09 theory to steady off-equatorial heating. Reference is made throughout the work to the AMC solutions in the framework of the SWM and the derivations of these solutions are given in appendix A. The model equations and their steady states are presented in section 2. In section 3 the steady solutions of the SWM are derived and compared to long time integrations of the time-dependent equations. The findings of this work are summarized and discussed in section 4.

2. Model equations and steady states

a. Model equations

Following AP09, the nondimensional equations of the axially symmetric, inviscid SWM of a thin layer of fluid overlaying a stationary layer on the spherical Earth with a source of mass (height/temperature) Q are

$$\dot{V} = -VV' - \frac{\mu}{1-\mu^2}(\alpha_\tau M^2 + V^2)$$
$$+ (1-\mu^2)(\alpha_\tau\mu - \alpha_g h') - I\frac{Q}{h}V, \qquad (1a)$$

$$\dot{M} = -VM' - I\frac{Q}{h}(M - 1 + \mu^2), \qquad (1b)$$

$$\dot{h} = -(hV)' + Q, \qquad (1c)$$

where h is the height, $\mu = \sin\phi$ (where ϕ denotes latitude), $V = v\cos\phi$ is the meridional velocity (v) times $\cos\phi$, and $M = \cos^2\phi - u\cos\phi$ is the component of absolute angular momentum (angular momentum hereafter) in the direction parallel to Earth's axis of rotation, where u is the zonal velocity component. The dot and prime denote derivatives with respect to time and μ, respectively. The source Q is a relaxation to a prescribed height h_f associated with differential solar heating:

$$Q = h_f - h; \qquad (1d)$$

$$h_f = 1 + h_1\left[1 - 2(\mu - \mu_0)^2\right], \qquad (1e)$$

where h_1 is the ratio between half the equator-to-pole height difference H_1 and the scale height H_0, and μ_0 is the latitude of maximal heating. This form of the radiative-equilibrium height follows the upper branch of the radiative forcing used by HH80 in the $\mu_0 = 0$ case, by LH88 for the $\mu_0 = $ const. case, and by Fang and Tung (1999) in the annually varying μ_0 case. A constant atmospheric relaxation time τ is used to scale the time t. The problem is completely prescribed by the nondimensional parameters μ_0 and by

$$\alpha_\tau = (\Omega\tau)^2; \quad \alpha_g = \frac{gH_0\tau^2}{a^2}; \quad h_1 = \frac{H_1}{H_0}, \qquad (1f)$$

where g denotes the gravitational constant and a and Ω are Earth's radius and rotational frequency, respectively. The flag I is given by

$$I(Q) = \begin{cases} 0; & Q \leq 0 \\ 1; & Q > 0 \end{cases}, \qquad (1g)$$

so that vertical momentum mixing with the stationary bottom layer is enabled in Eqs. (1a) and (1b) only when mass is injected into the upper layer. In addition, the following scales are used in nondimensionalizing the equations: u on Ωa, M on Ωa^2, v on a/τ, and h and h_f on H_0. Regularity at the poles [where $\mu = \pm 1$; see Eq. (1a)] yields the boundary conditions

$$V(\mu = \pm 1, t) = 0 = M(\mu = \pm 1, t). \qquad (1h)$$

Under typical conditions in the troposphere ($H_0 \approx 10$ km, $H_1 \approx 1.5$ km, and for $\tau \approx 2$–3 weeks), the values of the nondimensional parameters in (1f) are $\alpha_\tau \approx 10^4$, $\alpha_g \approx 10^4$, and $h_1 \approx 0.15$. A thermal Rossby number used in this work as well as in earlier works, given by

$$R_T = \frac{2\alpha_g h_1}{\alpha_\tau} = \frac{2gH_1}{\Omega^2 a^2}, \qquad (1i)$$

is the counterpart of the thermal Rossby number of HH80 and LH88; its typical value is 0.16.

b. SWM steady states

Steady solutions of the SWM are obtained by setting the lhs of Eqs. (1a)–(1c) equal to zero everywhere. As shown in AP09, the SWM has three steady states that follow the sign of the source Q. A *radiative-equilibrium* steady state corresponds to $Q = 0$, which is given by

$$V = 0; \qquad (2a)$$

$$M^2 = (1 - \mu^2)^2 [1 + 2R_T(1 - \mu_0/\mu)] \quad \text{and,} \quad (2b)$$

$$h = h_f. \qquad (2c)$$

This steady state is the counterpart of the radiative-equilibrium state of HH80 and LH88. Similarly, a *uniform-M* steady state is given by

$$V = \frac{\int (h_f - h)\, d\mu}{h}; \qquad (3a)$$

$$M = \overline{M} \quad \text{and} \qquad (3b)$$

$$h = h_0 + \frac{h_1}{R_T}\left(\mu^2 - \frac{\overline{M}^2}{1 - \mu^2}\right), \qquad (3c)$$

which exists for $Q < 0$ and is the counterpart of the angular momentum–conserving state of HH80 and LH88. Here $\overline{M}$ is the constant value of M in this region and h_0 is an integration constant [note that a term proportional to V^2/α_τ is neglected in Eq. (3c); see AP09]. Comparable expressions for these two steady states have been derived by Schneider (1987) on the equatorial beta plane and by Shell and Held (2004) for a small angle approximation of the Hadley cell width.

An additional $Q > 0$ (i.e., mass acquiring) steady state exists, which for terrestrial circulations is associated with the rising branch of the Hadley circulation in the tropics. The combination of Eqs. (1b) and (1c) yields

$$(MVh)' = Q(1 - \mu^2). \qquad (4)$$

Integrating the steady-state versions of Eqs. (1c) and (4) and setting the constants of integration equal to zero yields

$$M = \frac{\int Q(1 - \mu^2)\, d\mu}{\int Q\, d\mu} \leq 1. \qquad (5)$$

Since this bound ($M \leq 1$) equals the maximal value of M at the underlying stationary lower layer, Eq. (5) may be considered an extension to the inviscid SWM of Hide's theorem, which states that in a steady, axially symmetric atmosphere, M attains its maximum at the lower viscous surface (cf. HH80 and, in more detail, Plumb and Hou 1992). Equation (5) can also be generalized to a nonstationary lower boundary layer.

Assuming $u \approx 0$ in the steady-state version of Eq. (1a) (i.e., $M \approx 1 - \mu^2$) at the mass acquiring region yields

$$h' \simeq -\frac{1}{\alpha_g}\left[\frac{1 - \mu^2}{2}\left(\frac{V^2}{1 - \mu^2}\right)' + \frac{QV}{h}\right] \ll 1. \qquad (6)$$

For typical values of $\alpha_g \sim 10^4$, h may be assumed to be uniform there, which is not the case outside this region since u increases with latitude because of angular momentum conservation. Moreover, for $\alpha_g \gg 1$ the uniformity of h in the mass-acquiring region is guaranteed for any physically realistic source [i.e., $Q \sim O(1)$]. Thus, by requiring that h be uniform in the tropics, the mass-acquiring steady state can be approximated by

$$M = \frac{1}{V}\int V'(1 - \mu^2)\, d\mu; \qquad (7a)$$

$$h = \overline{h} = \text{const.}; \qquad (7b)$$

$$V = \frac{\int (h_f - \overline{h})\, d\mu}{\overline{h}}, \qquad (7c)$$

where $\bar{h}$ denotes the constant value of h in this region and Eq. (7a) is obtained by letting h be uniform in Eqs. (1c) and (5).

Since the global integral of Q must vanish in a steady state (to conserve the total mass of air in the atmosphere), a $Q > 0$ (mass acquiring) steady state in one region must be accompanied by the prevalence of a $Q < 0$ (mass depleting and angular momentum conserving) steady state in another region. Moreover, for physically realistic Q distributions, the width of the region where the $Q > 0$ steady state prevails must be comparable to that of the $Q < 0$ steady state.

In addition, as shown in AP09, regularity at the equator (for $\mu_0 \neq 0$) and Hide's theorem (for $\mu_0 = 0$) mandate that the radiative-equilibrium steady state ($Q = 0$) cannot prevail globally. Thus, any global steady state must consist of all three steady states described above.

The meridional uniformity of temperature (which follows from the vertical homogenization of the zonal wind by vertical mixing) in the tropics was also derived by Fang and Tung (1996) for two-dimensional Boussinesq models, such as the ones employed by HH80 and LH88. However, in contrast to the conclusion reached above regarding the prevalence of the $Q > 0$ (uniform-h) and $Q < 0$ (uniform-M) steady states in two separate regions (i.e., both M and h cannot be uniform in the same latitude region), Fang and Tung (1996) have also assumed uniformity of both angular momentum and temperature throughout the entire Hadley cell when deriving analytical solutions for a Hadley circulation that includes intense convection.

As shown by Fang and Tung (1996), the weak temperature gradient and the vertical homogeneity of the zonal wind are consistent with the thermal wind balance and both are observed in the rising branch of the Hadley circulation in the zonally averaged tropics. The vertical homogeneity of the zonal wind, however, means that the upper branches of the tropic Hadley circulation are in communication with the viscous bottom boundary. Therefore, angular momentum conservation cannot coincide with strong mixing, which explains (regardless of the effect of eddies) why it is not observed at the rising branch of the Hadley circulation in the zonally averaged tropics [e.g., Vallis 2006, his Fig. 11.2, where $u \approx$ const. $< \sin^2(\phi)/\cos(\phi)$ in the rising branch of the Hadley circulation].

3. SWM steady-state solutions for constant μ_0

a. Analytical solutions for the SWM attractor sets

As depicted schematically in Fig. 1, steady solutions of the SWM entail a three-region paradigm: (i) a tropical (region I) mass-acquiring, uniform-h region given by Eqs. (7a)–(7c), whose winter and summer boundaries are $\bar{\mu}_w$ and $\bar{\mu}_s$, respectively; (ii) a subtropical (region II)
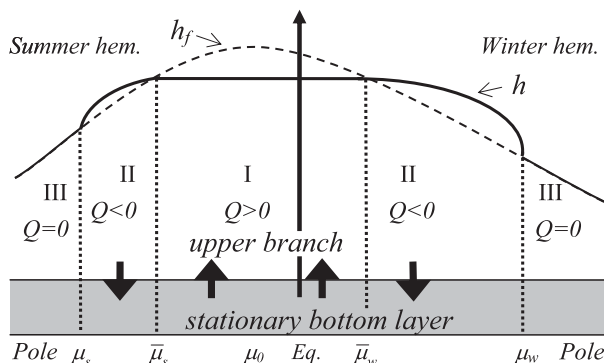

FIG. 1. A schematic depiction of the communication of mass between the upper and lower branch of the circulation and the meridional profiles of h_f and h of the SWM illustrating the relative locations of μ_w and μ_s, the poleward edges of the winter and summer cells, respectively; $\bar{\mu}_w$ and $\bar{\mu}_s$, the winter and summer edges of the mass acquiring region, respectively; and μ_0, the latitude of maximal heating. The designation of the regions follows the sign of $Q = h_f - h$. Region I is a tropical, mass-acquiring ($Q > 0$), uniform-h region; region II is a subtropical, mass depleting ($Q < 0$) uniform-M region; and region III is a steady radiative-equilibrium region ($Q = 0$).

mass-depleting, uniform-M region given by Eqs. (3a)–(3c) bounded by μ_w and μ_s in its winter and summer boundaries, respectively; and (iii) an extratropical (region III) radiative-equilibrium region given by Eqs. (2a)–(2c) where $Q = 0$. In addition, we assume that the tropics host winter and summer cells, connected at μ_1 (the latitude where V changes sign) on the summer side of the equator (where $\mu\mu_0 > 0$). The functional form of V, M, and h in this configuration is referred to as the attractor set, denoted by $[V_A(\mu), M_A(\mu), h_A(\mu)]$ and defined as the stable steady states of the time-dependent equations that are reached by phase space trajectories after long times. As in the solutions of HH80 and LH88, these attractor sets involve a discontinuity in M_A at the transition points between the uniform-M and radiative-equilibrium regions.

The attractor sets of the SWM $[V_A(\mu), M_A(\mu), h_A(\mu)]$ are obtained in the following manner: requiring the continuity of h at $\bar{\mu}_s$, $\bar{\mu}_w$, μ_s, and μ_w yields

$$\bar{\mu}_s = 2\mu_0 - \bar{\mu}_w, \tag{8}$$

$$\overline{M}_q^2 = (1 - \mu_q^2)(1 - \bar{\mu}_q^2)\left(1 + 2R_T - \frac{4R_T\mu_0}{\mu_q + \bar{\mu}_q}\right), \tag{9}$$

and

$$h_{0,q} = 1 + h_1 - \frac{h_1}{R_T}\left[\mu_q^2 + 2R_T(\mu_q - \mu_0)^2 - \frac{\overline{M}_q^2}{1 - \mu_q^2}\right], \tag{10}$$

where the subscript q denotes either w or s and where $h_{0,q}$ and $\overline{M}_q$ denote the constant of integration and the value of M in the uniform-M regions, respectively. Imposing $V_A(\mu_1) = 0$ and $\overline{h}(\bar{\mu}_q) = h_f(\bar{\mu}_q)$, V_A in region I is explicitly calculated from Eq. (7c):

$$V = \text{sign}(\mu_q) \frac{2h_1}{\overline{h}} \int_{\mu_1}^{\mu} \left((\mu - \mu_0)^2 - (\bar{\mu}_q - \mu_0)^2 \right) d\mu. \quad (11)$$

Accordingly, using Eq. (7a) M_A in region I is explicitly given by

$$M = 1 - \mu^2 + \frac{\left\{ \begin{array}{l} \frac{1}{3}\left[(\mu_1 - \mu_0)^3 + \mu_0^3 - 3\mu_1(\bar{\mu}_q - \mu_0)^2 \right](\mu^2 - \mu_1^2) \\ + \frac{2}{3}(\bar{\mu}_q^2 - 2\mu_0\bar{\mu}_q)(\mu^3 - \mu_1^3) + \frac{1}{2}\mu_0(\mu^4 - \mu_1^4) - \frac{2}{15}(\mu^5 - \mu_1^5) \end{array} \right\}}{(\bar{\mu}_q - \mu_0)^2(\mu - \mu_1) + \frac{1}{3}\left[(\mu_1 - \mu_0)^3 - (\mu - \mu_0)^3 \right]}. \quad (12)$$

From Eq. (12) we obtain for $\overline{M}_q$

$$\overline{M}_q = 1 + \frac{\frac{1}{2}\mu_0\mu_1^4 + \frac{1}{3}\mu_1^3\bar{\mu}_q^2 - \frac{2}{15}\bar{\mu}_q^5 - \frac{1}{5}\mu_1^5 + \frac{1}{6}\mu_0\bar{\mu}_q^4 - \frac{2}{3}\mu_0\bar{\mu}_q\mu_1^3}{\frac{1}{3}\mu_1^3 + \frac{2}{3}\bar{\mu}_q^3 - \mu_1\bar{\mu}_q^2 - \mu_0(\mu_1 - \bar{\mu}_q)^2}. \quad (13)$$

Finally, the conservation of mass in each cell is given by

$$\int_{\mu_1}^{\bar{\mu}_q} (\overline{h} - h_f) \, d\mu + \int_{\mu_{\overline{q}}}^{\mu_q} (h - h_f) \, d\mu = 0, \quad (14a)$$

which yields the explicit relationship

$$0 = \frac{\overline{M}_q^2}{1 + 2R_T} \left\{ \frac{\mu_q - \bar{\mu}_q}{1 - \mu_q^2} - \frac{1}{2} \ln\left[\frac{(1 + \mu_q)(1 - \bar{\mu}_q)}{(1 - \mu_q)(1 + \bar{\mu}_q)} \right] \right\} + \mu_q^2\bar{\mu}_q - \frac{2\mu_q^3 + \bar{\mu}_q^3}{3}$$
$$+ \frac{2R_T}{1 + 2R_T} \left\{ \mu_1\bar{\mu}_q^2 - \frac{2\bar{\mu}_q^3 + \mu_1^3}{3} + \mu_0\left[(\mu_q - \bar{\mu}_q)^2 + (\mu_1 - \bar{\mu}_q)^2 \right] \right\}. \quad (14b)$$

Note that Eq. (14) differs from the analogous expression in Polvani and Sobel (2002, their Eq. 13), since, like Fang and Tung (1996), they assume that h is uniform (to first order) over the entire cell and not only in the inner, strong mixing region as in the present theory. In addition, while deviations from angular momentum conservation are allowed in the simplified model used by Polvani and Sobel (2002), these are attributed to a form of internal friction and not to vertical advection of momentum. Equations (8), (9), and (14b) form a set of five nonlinear transcendental algebraic equations for the five unknowns, μ_q, $\bar{\mu}_q$ (recall that the subscript q stands for s and w), μ_1, with $\overline{M}_q$ given by Eq. (13). It is readily verified that by setting μ_0 and μ_1 equal to zero and $\bar{\mu}_w = -\bar{\mu}_s$, $\mu_w = -\mu_s$, one derives the analogous expressions of the equinoctial case given in AP09.

The attractor sets of the SWM are determined by two parameters only: μ_0 and R_T. Figure 2 shows the dependence of the relative locations of μ_q (solid), $\bar{\mu}_q$ (dashed), and μ_1 (dotted) on R_T for ϕ_0 [$=\arcsin(\mu_0)$] $= -3°$ (top)

and $-6°$ (bottom). It is observed that the relative locations of the regions' boundaries (and hence the subtropical jets) are primarily determined by R_T, as in the AMC solutions (cf. with Fig. A2a).

From Eq. (12) it is possible to solve explicitly for the location and strength of the tropical easterlies. Figure 3 displays the location ϕ_E (left panel) and strength u_E (right panel) of the tropical easterlies, defined as the location and value, respectively, of the tropical minima in the zonal velocity, which are derived from Eq. (12). The dependence of the easterlies' location and strength on ϕ_0 are plotted for $R_T = 0.1$ (dotted), 0.25 (dashed), and 0.16 (solid), which represent the range of terrestrially acceptable R_T values (0.1–0.25) and its commonly used value (0.16). Since for $\mu_0 \neq 0$ M is not symmetric about the equator, the attractor sets of the SWM include easterlies that peak on the summer side of the equator (i.e., off the equator), unlike the nearly inviscid solutions of LH88 (see their Fig. 6), where strong easterlies peak on the equator. For terrestrially acceptable values of μ_0 and R_T these
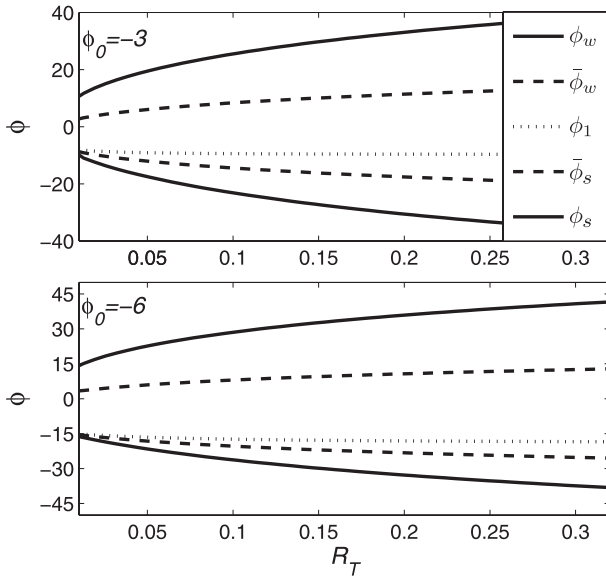
FIG. 2. The dependence on the thermal Rossby number R_T of ϕ_w (solid; positive), ϕ_s (solid; negative), $\bar{\phi}_w$ (dashed; positive), $\bar{\phi}_s$ (dashed; negative) and ϕ_1 (dotted; negative), corresponding to μ_w, μ_s, $\bar{\mu}_w$, $\bar{\mu}_s$, and μ_1, respectively, and denoting the winter and summer latitudes of the subtropical jets, the boundaries of the mass acquiring region and the latitude where the winter and summer cells connect, respectively, for ϕ_0, the latitude of maximal heating (corresponding to μ_0) of (top) $-3°$ and (bottom) $-6°$.

easterlies do not exceed 25 m s^{-1} in the present theory. The dependence of the location of the tropical easterlies on μ_0 matches the result of Fang and Tung (1999, their Fig. 3).

The maximal value of V in each cell, approximated by $V(\bar{\mu}_q)$ (where Q changes sign), is often regarded as a measure of the cell strength. Using Eqs. (8) and (11) and keeping only leading-order powers, one obtains the following simple approximation for the cell strength ratio (i.e., the ratio between the cell strength in the summer and northern hemispheres) $K_V^{s/w}$:

$$K_V^{s/w} \simeq \frac{\bar{\mu}_s - \mu_1}{\mu_1 - \bar{\mu}_w} = \frac{\bar{\mu}_s - \mu_1}{\mu_1 - 2\mu_0 + \bar{\mu}_s} = \frac{2\mu_0 - \bar{\mu}_w - \mu_1}{\mu_1 - \bar{\mu}_w}. \tag{15}$$

The dependence of this simple approximation of $K_V^{s/w}$ on ϕ_0 for different values of R_T (e.g., Fig. 3) is shown in Fig. 4. The cell strength ratio $K_V^{s/w}$ equals 1 for equinoctial heating and vanishes nonlinearly with the increase of $|\phi_0|$ (though not as steeply as in the AMC solutions of LH88) at a rate that decreases with R_T.

b. Initial conditions and numerical integrations

Time integrations of system (1a)–(1c) were performed using a staggered-grid (where h is staggered from V and M) leapfrog scheme with a Robert–Asselin time filter
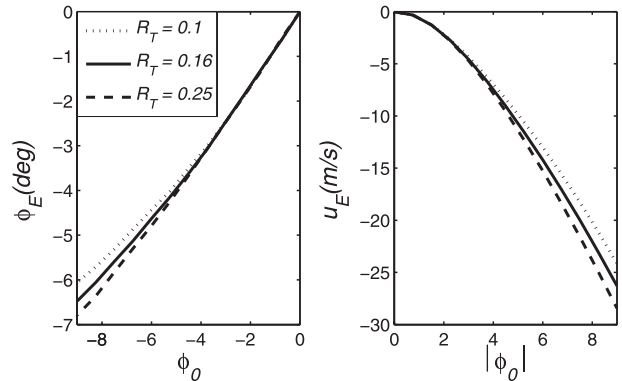

FIG. 3. The dependence of the (left) latitude ϕ_E (corresponding to μ_E) and (right) strength u_E (m s^{-1}) of the tropical easterlies on the latitude of maximal heating, ϕ_0 [$=\arcsin(\mu_0)$] for three values of R_T, the thermal Rossby number. The values $R_T = 0.1$ (dotted) and $R_T = 0.25$ (dashed curves) represent two extremes of terrestrially acceptable values; $R_T = 0.16$ (solid curve) represents its typical terrestrial value. The strength and location of the tropical easterlies depend primarily on ϕ_0, and the location, ϕ_E, has the same sign as ϕ_0.

($\alpha = 0.001$), identical to the one used in AP09. A detailed description of the numerical method, the scaling, and choice of parameters is found in AP09.

The attractor set of the SWM depends very weakly on the choice of initial conditions. Except for integrations initiated from a perturbation of (i.e., near) the radiative-equilibrium state described by Eqs. (2a)–(2c) in which a global radiative-equilibrium steady state was reached after long times for $\mu_0 = 0$ [an off-equatorial global radiative equilibrium state cannot exist due to the singularity on the equator in Eq. (2a)], all physically acceptable
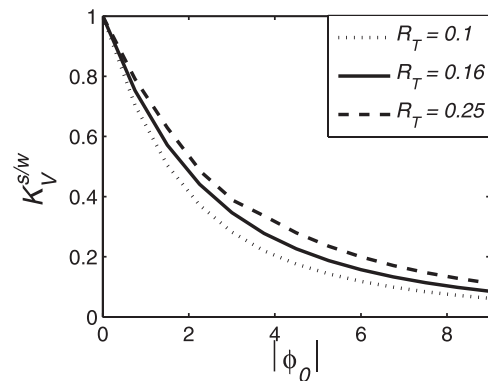

FIG. 4. The ratio between the strengths of the summer and winter cells, $K_V^{s/w}$, as a function of the latitude of maximal heating, ϕ_0 [$=\arcsin(\mu_0)$], for three values of R_T. The values $R_T = 0.1$ (dotted curve) and $R_T = 0.25$ (dashed curve) represent two extremes of terrestrially acceptable values; $R_T = 0.16$ (solid curve) represents a typical terrestrial value. Note that $K_V^{s/w}$ strongly decreases with $|\phi_0|$ and increases weakly with R_T. The summer cell strength is about 10% of the winter cell strength for approximate values of $|\phi_0|$ at solstice on Earth.
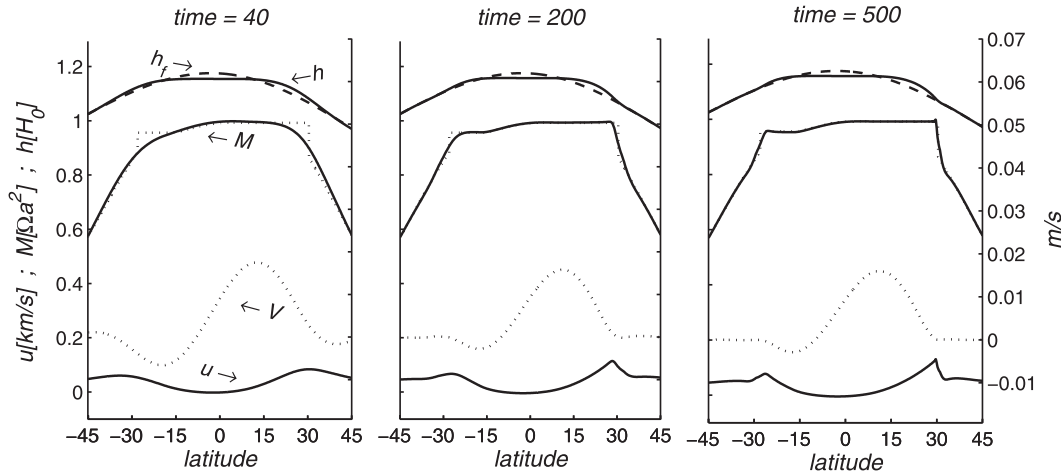
FIG. 5. Numerical solutions of the time-dependent SWM at $t = 40$, 200, and 500. The system is initiated by $M = \cos(\phi)$, $V(\phi) = 0$, and $h(\phi) = 1$. The parameters used are $\phi_0 = -3°$ (i.e., $\mu_0 = -0.052$), $\tau = 20$ days, and $h_1 = 0.175$ so that $\alpha_g = 18\tau^2 = 7200$, $\alpha_\tau = (2\pi\tau)^2 = 1.6 \times 10^4$, and $R_T = 0.16$. The dimensional scales for h (H_0, top solid), h_f (top dashed), M (Ωa^2, solid), M_A(dashed), and u (km s^{-1}, solid) are given on the left ordinate. The dimensional scale for V (m s^{-1}, dashed) is given on the right ordinate. The three regions of the steady attractor set—a tropical, uniform-h mass acquiring region; a subtropical, mass-depleting uniform-M region; and an extratropical tropical radiative-equilibrium region—are evident as early as $t = 40$ and are fully established at $t = 200$; further integration to $t = 500$ only further strengthens this three-region structure. At $t > 200$, the numerically integrated M is distinguishable from the analytically obtained M_A only at the ever-narrowing transition zones between the uniform-M and radiative-equilibrium regions. The tropical easterlies peak on the summer side of the equator. The meridional range in the abscissa is truncated at 45°, poleward of which radiative equilibrium is fully established at $t = 40$.

initial conditions yielded the steady states predicted by the three-region paradigm.

It is clear from Fig. 2 that μ_1 is located in the strong mixing region. From Eq. (1b), at steady state, since $V(\mu_1) = 0$, $u \cos\phi(= M - 1 + \mu^2)$ must vanish at that point, even though no friction was added to the equations. This result is consistent with the assumptions of LH88, except that unlike their AMC solutions, in the present theory M is not uniform there. This result is slightly different from the one obtained by Schneider (1987), who showed that in the absence of vertical advection of momentum, u must physically vanish at that point because Eq. (1b) may be considered as the $c \to 0$ limit of a drag term, $cu \cos\phi(c < 0)$ added to its rhs. The difference between the two approaches lies in the fact that in the presence of vertical advection of momentum u must equal the velocity of the bottom layer (stationary in this case). Therefore, for a nonstationary bottom layer, the second term on the rhs of Eq. (1b) becomes $-I(Q/h)(M - 1 + \mu^2 - U_0)$, where U_0 denotes $u \cos\phi$ at the bottom layer, in which case $u(\mu_1)$ does not vanish.

A time series of the numerically integrated SWM for the parameters $\phi_0 = -3°$ and $R_T = 0.16$ and the initial conditions, $M = 1 - \mu^2$, $V = 0$, and $h = $ const. is given in Fig. 5. At $t > 200$, the functional form of the analytically obtained M_A (dotted) is distinguishable from the numerically integrated M (solid) only at the transition zone

between the uniform-M and radiative-equilibrium regions. Similar results were encountered in a wide range of initial conditions. Isolated singular extrema in M may appear at the poleward boundary of the winter cell because M is materially conserved there, as can be (hardly) seen in Fig. 5. The isolated singular extrema do not affect the steady attractor sets elsewhere (the origin of the isolated singular extrema is elaborated upon in appendix A). For comparison, a similar numerical integration of the SWM with the same parameters and initial conditions as Fig. 5 but in which vertical advection of momentum is disabled [i.e., $I = 0$ everywhere in Eqs. (1a) and (1b), corresponding to AMC solutions] is shown in Fig. 6. A more pronounced singular extremum is seen in the poleward boundary of the winter cell because in the absence of mixing, M is materially conserved throughout the circulation cell. Note that while in the integrations corresponding to the three-region paradigm (Fig. 5) physically realistic easterlies form on the summer side of the equator and the cell strength ratio (i.e., the ratio of the summer and winter cell strengths) is about 0.3, in the results corresponding to AMC solutions (Fig. 6) strong equatorial easterlies form and the summer cell nearly vanishes. In addition, comparing the three-region, off-equatorial, and equinoctial solutions shown in Fig. 5 here and Fig. 9 of AP09 with their AMC counterparts, Fig. 6 here and Fig. 3 of AP09, demonstrates the enhanced deviation from
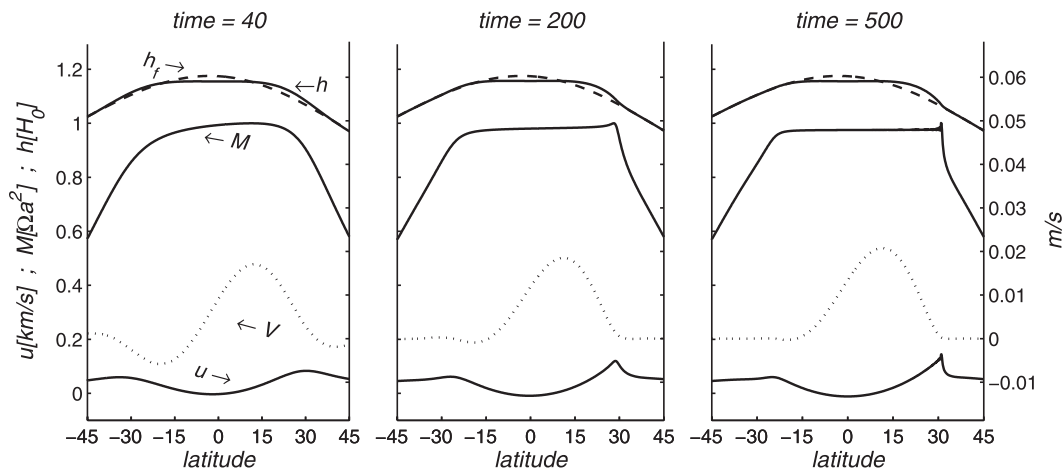
FIG. 6. As in Fig. 5, but with vertical advection of momentum from the underlying bottom layer missing from the SWM—that is, the SWM analog of the AMC solution (sketched in Fig. A1). The initial conditions and values of model parameters are identical to those of Fig. 5, which yields $B_E = 0.76$ and $B_S = -0.013$ for this model. A tropical, uniform-M region is established as early as $t = 200$, at which time a singular $M = 1$ point starts to form at the poleward boundary of the winter cell because of the extremum principle. The $M < 1$ uniform-M region results from $B_E > B_0$ for the above choice of parameters and it overrides the $M = 1$ initial condition at the equator. These features persist and sharpen through $t = 500$.

angular momentum uniformity as the heating shifts away from the equator, as was noted by LH88.

4. Summary and discussion

The angular momentum–conserving (AMC) solutions for the upper branch of the ideal Hadley circulation of HH80 and LH88 are identical to the solutions of the forced SWM when vertical advection of momentum from the underlying boundary layer is disabled (appendix A). This relationship between the forced SWM without vertical advection of momentum and the AMC solutions enables a comparison between the latter solutions and those of the forced SWM *with* vertical advection of momentum. Thus, the three-region paradigm described in the present study can be compared to the two-region paradigm of AMC solutions in an Eulerian (inviscid) framework that is free of any spurious effects of the rigid lid assumption (Walker and Schneider 2005). The inter-model comparison is best carried out by comparing the predictions of each of these models with axially symmetric simulations (e.g., Walker and Schneider 2005; HH80) and with zonally averaged observations of the atmosphere. Comparing the observations and simulations with AMC solutions highlights the following shortcomings:

(i) AMC solutions predict a cross-hemispherical uniform-M region that does not exist in axially symmetric simulations. Instead, in axially symmetric simulations, vertical advection of momentum at the tropics (that can extend to over half the total

circulation width) causes nonuniformity of the angular momentum there (e.g., Walker and Schneider 2005). Thus, the uniform-M region prevails only at the outer portions of the Hadley circulation (e.g., HH80, their Fig. 6).

(ii) Off-equatorial AMC solutions predict strong temperature (height) gradients at the tropics, which are not observed even in winter and were not encountered in axially symmetric simulations such as LH88. In addition, the off-equatorial heating AMC solutions predict unphysical strong easterlies that peak right on the equator even for small displacements of the latitude of maximal heating whereas the observed and simulated equatorial jets are weak and peak away from the equator.

(iii) The ratio of the summer and winter Hadley circulation strengths in the AMC solutions is sensitive to small displacements from the equator of the latitude of maximal heating (ϕ_0). In addition, for the same thermal Rossby number R_T, the winter Hadley cell produced by off-equatorial heating is much stronger than either of the cells of equinoctial heating even for small μ_0, so AMC solutions predict an annually (summer and winter) averaged Hadley circulation that is much stronger than the annually averaged circulation of equinoctial heating even for small μ_0. This prediction is in contrast to the observed (Dima and Wallace 2003) and simulated (Walker and Schneider 2005) annually averaged Hadley circulation strength, which is up to twice the equinoctial heating Hadley circulation strength.

In contrast to the predictions of the two-region AMC solution paradigm, the new features of the solutions that result from the three-region paradigm of the present study are the following:

(i) The rising branch of the Hadley circulation is described as a strong vertical mixing region in which the temperature gradient is very weak and angular momentum is not conserved. The temperature gradients drastically increase with latitude in the neighboring angular momentum conserving regions that lie poleward of this region.

(ii) The angular momentum conserving and strong mixing regions have similar meridional extents, as observed in two-dimensional simulations.

(iii) Off-equatorial heating produces physically realistic easterlies that peak on the summer side of the equator and are close to it.

(iv) The sensitivity of the Hadley circulation strength to small values of μ_0 in the three-region paradigm solutions is reduced compared to that of the AMC solutions, and is therefore in better agreement with the observed and simulated circulation.

The above comparison reaffirms that the shortcomings of the AMC solutions listed here are solely due to the misrepresentation of vertical advection of momentum in these solutions (i.e., they do not result from friction or from the rigid lid assumption). Furthermore, in contrast to the two-region paradigm of the AMC solutions, the incorporation of vertical advection of momentum mandates solutions that follow a three-region paradigm: a tropical, mass-acquiring, weak temperature gradient region; subtropical mass-depleting, uniform-M regions (in which the temperature gradient is not weak); and extratropical radiative-equilibrium regions. In addition, since the source of mass changes sign between the mass-acquiring and mass-depleting regions, these regions must be of comparable extent (for physically realistic distributions of the source) for the total mass to be conserved.

A direct consequence of the three-region paradigm advocated in the present study is that the tropical, strong mixing region is well described by letting h (viewed as the temperature) be uniform there in steady state. Using this approximation (as well as the trivial continuity of M and h and conservation of mass), the locations of the boundaries of the three steady-state regions are explicitly given by the roots of a set of nonlinear transcendental algebraic equations [i.e., Eqs. (8), (9), and (14b)]. In addition, the functional form of V, M, and h within each of these regions is explicitly given by Eqs. (2), (3), and (7). Our numerical integrations of the time-dependent equations for long times indicate that the solutions obtained by the uniform-h approximation accurately predict the steady

attractor sets of the model. The uniformity of h in the tropical strong mixing region results from the vanishing zonal winds there [see Eq. (6)]. However, as shown in Fig. 3, the equatorial easterlies strengthen as the location of maximal heating (ϕ_0) shifts away from the equator. Appreciable deviations from uniform h in the tropical strong mixing region in our numerical integrations of the time-dependent equations for long times are observed for $\phi_0 > 9°$. As in the AMC solutions, the three-region paradigm solutions are determined by the thermal Rossby number and the latitude of maximal heating.

The width of the Hadley circulation and the relative locations of the subtropical jets and their amplitudes are not well captured in both the AMC solutions and the present three-region solutions. These shortcomings of the steady-state solutions are attributed to the fact that the atmosphere is never at a steady state and to the absence of diffusion and eddies that are driven partly by the subtropical jets. However, in contrast to the predictions of the AMC and the three-region solutions in the midlatitudes, physically realistic easterlies are predicted by the three-region solutions in the tropical strong mixing region, suggesting that eddies have a weak influence on the circulation there. This result is in agreement with Lee (1999), who showed that momentum fluxes in the deep tropics are dominated by the transient meridional circulations. The influence of eddies on the Hadley circulation strength may be clarified by further investigation of the time-dependent properties of the annually varying idealized circulation.

APPENDIX A

AMC Solutions for Constant μ_0 in the SWM

a. The extremum principle and initial conditions

The AMC solutions in the framework of the SWM are obtained by disabling vertical advection of momentum (AP09). Steady states are therefore obtained by setting the lhs of Eqs. (1a)–(1c) to zero and setting $I = 0$ everywhere. By setting $I = 0$ everywhere, Eq. (1b) simply states the material conservation of M. It is well known that extremum values of materially invariant quantities are conserved (see appendix B for a derivation of the extremum principle in the context of the present SWM), so that the steady states of the SWM (without vertical
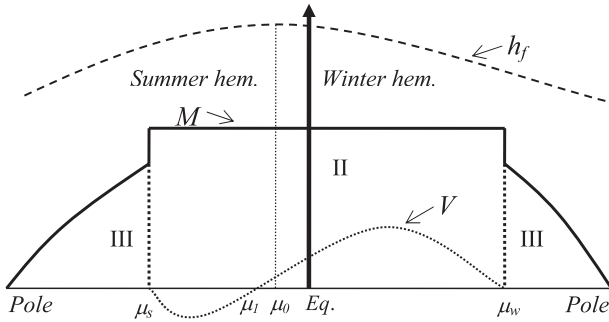
FIG. A1. A schematic depiction of the meridional profiles of the angular momentum M, the meridional velocity V, and the forcing height h_f of the steady SWM without vertical advection of momentum, representing the SWM counterpart of AMC solutions. Note that M, V, and h_f are all plotted on the same vertical axis in arbitrary units, illustrating the relative locations of μ_w, the poleward edge of the winter cell; μ_s, the poleward edge of the summer cell; μ_1, the latitude at which the winter and summer cells connect (and where V changes sign); and μ_0, the latitude of maximal heating. The designation of the two steady-state regions is as follows: a tropical uniform-M region (II) and an extratropical radiative-equilibrium region (III).

advection of momentum) are expected to strongly depend on initial conditions. The initial conditions considered in this work include only initial distributions of M with a single extremum value (point or section) from which M decreases monotonically to the poles. For similar initial conditions, the extremum principle was used by AP09 in the equinoctial case ($\mu_0 = 0$) to determine that the value of M at the equator (where $V = 0$) is a constant set by the initial conditions. When the hemispheric symmetry is broken by off-equatorial heating, the maximal value of M remains a constant set by the initial conditions, but its *location* is no longer fixed to the equator. The values of M that are physically allowed by Hide's theorem have to satisfy $M \le 1$.

b. Analytical AMC solutions in the framework of the forced SWM

We assume that at steady state the circulation is composed of a tropical uniform-M region and extratropical radiative-equilibrium regions that connect to the tropical region at transition points in the winter (μ_w) and summer (μ_s) hemispheres. Figure A1 is a schematic depiction of the meridional profile of M_A (solid), V_A (dotted), and h_f (dashed). At the winter and summer transition points M_A is discontinuous. The transition points mark the limit approached by the time-dependent equations, in which an ever-narrowing unsteady transition region exists between the steady regions (AP09).

We solve for the steady attractor sets $[V_A(\mu), M_A(\mu), h_A(\mu)]$ by requiring the continuity of h at both μ_s and μ_w, which yields the relationship

$$B_E = (1 - \mu_w^2)(1 - \mu_s^2)(1 - 2B_S/(\mu_w + \mu_s)), \quad (A1)$$

where the steady-state parameters B_E and B_S are defined by

$$B_E = \frac{\overline{M}^2}{1 + 2R_T} \quad \text{and} \quad (A2a)$$

$$B_S = \frac{2R_T \mu_0}{1 + 2R_T}, \quad (A2b)$$

and in which $\overline{M}$ is a constant set by the initial conditions (due to the extremum principle). On the Earth the relevant values of these parameters are $0.6 < B_E < 0.8$ and $|B_S| < 0.06$. In addition, we require conservation of mass in each cell:

$$\int_{\mu_1}^{\mu_q} (h_f - h) \, d\mu = 0, \quad (A3)$$

where μ_q denotes either μ_s or μ_w. Explicit integration of Eq. (A3) for the summer and winter cells yields

$$B_E \left\{ \frac{\mu_1 - \mu_s}{1 - \mu_s^2} - \frac{1}{2} \ln\left[\frac{(1 + \mu_1)(1 - \mu_s)}{(1 - \mu_1)(1 + \mu_s)} \right] \right\}$$
$$= \mu_s^2(\mu_1 - \mu_s) - \frac{\mu_1^3 - \mu_s^3}{3} + B_s(\mu_1 - \mu_s)^2 \quad (A4a)$$

and

$$B_E \left\{ \frac{\mu_w - \mu_1}{1 - \mu_s^2} - \frac{1}{2} \ln\left[\frac{(1 + \mu_w)(1 - \mu_1)}{(1 - \mu_w)(1 + \mu_1)} \right] \right\}$$
$$= \mu_s^2(\mu_w - \mu_1) - \frac{\mu_w^3 - \mu_1^3}{3}$$
$$+ B_s(\mu_w - \mu_1)(\mu_w + \mu_1 - 2\mu_s), \quad (A4b)$$

respectively, where h is given by Eq. (3c). It is readily shown that setting $\mu_0 = 0$, $\mu_1 = 0$, and $\mu_s = -\mu_w = \mu_J$ yields

$$B_E \left[\frac{\mu_J}{1 - \mu_J^2} - \frac{1}{2} \ln\left(\frac{1 + \mu_J}{1 - \mu_J} \right) \right] = \frac{2}{3} \mu_J^3, \quad (A5)$$

which is the equation obtained by AP09 for μ_J, the hemisphere-independent transition point (and the location of the subtropical jet) in the equinoctial case. As was shown in AP09, the roots of Eq. (A5) are identical to the roots of Eq. (17) in HH80 for $\overline{M} = 1$. Similarly, the roots of Eqs. (A1) and (A4) are identical to the AMC solutions of LH88 upon substituting $\overline{M} = 1 - \mu_1^2$ into Eqs. (A1) and (A4).

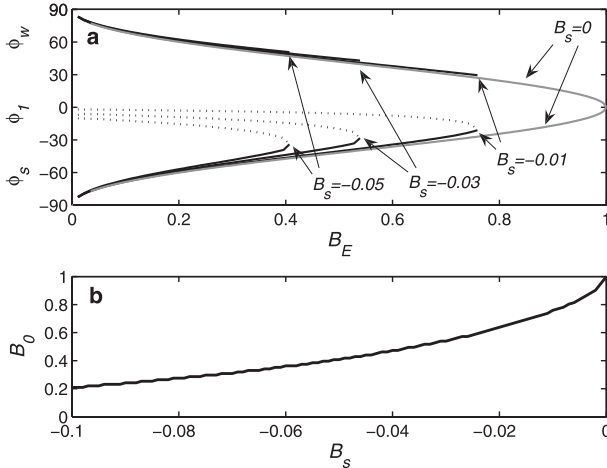These results echo those of HH80 and LH88 in the SWM framework. However, whereas in the SWM $\overline{M}$ is

FIG. A2. (a) The dependence of ϕ_w (solid curve, positive values), ϕ_s (solid curve, negative values), and ϕ_1 (dashed curve, negative values) on B_E [$= \overline{M}^2/(1 + 2R_T)$] for $B_S = 0$ (equinoctial case), -0.01, -0.03, and -0.05 [where $B_S = 2R_T\mu_0/(1 + 2R_T)$]. Here ϕ_w, ϕ_s, and ϕ_1 denote the winter and summer latitudes of the subtropical jets and the latitude where the winter and summer cells connect, respectively. The corresponding values of μ_w, μ_s, and μ_1 are related to ϕ_w, ϕ_s, and ϕ_1, respectively, by the general $\mu = \sin(\phi)$ relation. (b) The dependence of B_0 (which denotes the cutoff value of B_E at which $\mu_s = \mu_1$) on B_S. Physically realistic attractor sets exist only for $B_E \leq B_0$.

a parameter whose value is set by the initial conditions, in the AMC solutions of LH88 $\overline{M}$ is determined by requiring that the zonal velocity vanish at the separation point between the summer and winter cells [i.e., $u(\mu_1) = 0$]. It is therefore not guaranteed that AMC solutions in the SWM exist for all initial conditions. The dependence of solutions to Eqs. (A1) and (A4) on B_E for different values of B_S (including the equinoctial, $B_S = 0$ case) is shown in Fig. A2a. A cutoff value of B_E at which the summer cell vanishes (i.e., $\mu_1 = \mu_s$) exists for each B_S. This cutoff value, denoted B_0, is shown in Fig. A2b as a function of B_S. AMC solutions of the attractor sets that follow the two-region paradigm described in Fig. A1 exist only for $B_E \leq B_0$ (i.e., below the curve displayed in Fig. A2b). In Fig. A2, $B_E \geq 0$ and $B_S \leq 0$ so that $\mu_w \geq 0$ and μ_1 and $\mu_s \leq 0$. This phase space is symmetric with respect to the sign of μB_S.

Let $(\mu_s^*, \mu_1^*, \mu_w^*)$ and (μ_s, μ_1, μ_w) denote the solutions of Eqs. (A1) and (A4) for the sets (B_E^*, B_S^*) and (B_E, B_S), respectively. Then the results shown in Fig. A2 imply that for

$$|B_S^*| > |B_S|, \quad |\mu_w^*| > |\mu_w| > |\mu_J|, \quad |\mu_s^*| < |\mu_s| < |\mu_J|,$$
$$|\mu_1^*| > |\mu_1| \quad \text{and} \quad B_0^* < B_0 \tag{A6a}$$

while for

$$B_E^* > B_E, \quad |\mu_w^*| < |\mu_w|, \quad |\mu_s^*| < |\mu_s|, \quad \text{and}$$
$$|\mu_1^*| > |\mu_1|. \tag{A6b}$$

In addition, it is apparent from Fig. A2a that the relative locations of μ_s, μ_1, and μ_w are determined primarily by B_E.

c. Initial conditions and numerical integrations

The extremum principle mandates that for the attractor sets determined by solutions of Eqs. (A1) and (A4), the value of M in the uniform-M region must equal the single maximum of M in the initial conditions, so that B_E is set by the initial conditions. Our numerical results indicate that initial conditions for which there exists a μ_1 in the solutions of Eqs. (A1) and (A4) that satisfies

$$\mu_1 \in \mu_x; \quad \overline{M} = M_x, \quad B_E < B_0, \tag{A7}$$

where M_x denotes $\max[M(0, \mu)]$ and μ_x denotes the interval in which $\overline{M} = M_x$, yield the AMC attractor sets determined by the solutions of Eqs. (A1) and (A4) and shown in Fig. A2a. For initial conditions that do not satisfy condition (A7), the maximum in M travels to the winter hemisphere where it becomes (asymptotically) an isolated extremum point at μ_w. The uniform-M region that forms on its equatorward side has $\overline{M} < M_x$. For example, for $R_T = 0.16$ and $\overline{M} = 1$, the summer cell vanishes ($\mu_1 = \mu_s$) for $|\mu_0| = 2.4°$ (or $|B_S| \approx 0.01$). For $|\mu_0| > 2.4°$ (i.e., $B_E > B_0$), the system evolves into a combination of an AMC attractor set that satisfies $B_E \leq B_0$ and an unphysical isolated singular extremum point at μ_w at which $\overline{M} = 1$. Figure 6 is a time series of the above example, initiated with a single maxima at the equator [$M(0, 0) = 1$] and $\mu_0 = -3°$. The isolated singular $M = 1$ point and the $M < 1$ uniform-M region are clearly observed. Since at long times such singular extremum points are inevitably either numerically or physically diffused, attractor sets that include these points are unphysical artifacts resulting from the absence of viscosity in the SWM.

APPENDIX B

1D Extremum Principle

In this appendix we wish to derive an extremum principle for all 1D materially conserved quantities, such as angular momentum in the SWM.

Consider a materially conserved quantity E, such that

$$\dot{E} + VE' = 0. \tag{B1}$$

Let $-1 \leq \mu_x(t) \leq 1$ be the (time dependent) point where the extremum of E in the interval $[-1, 1]$ is located. From Eq. (A1) we obtain

$$\dot{E}\big|_{\mu_x} = -V\underbrace{E'\big|_{\mu_x}}_{=0} = 0. \tag{B2}$$

Let $E_x = E[\mu_x(t)]$ be the value of E at the extremum point. The total derivative of E there is given by

$$\frac{dE_x}{dt} = \underbrace{\frac{\partial E_x}{\partial t}}_{=0} + \underbrace{\frac{\partial E}{\partial \mu}\bigg|_{\mu_x}}_{=0} \frac{\partial \mu_x}{\partial t} = 0. \tag{B3}$$

Thus, an extremum value of E is constant in time, propagating in the domain $[-1, 1]$ at a velocity $V(\mu_x(t))$. Conversely, extrema that are not present at $t = 0$ cannot exist at $t > 0$.

Next, consider a uniform distribution of E over a subinterval $[\mu_-(t)\ \mu_+(t)]$ and let E_x be the value of E in this subinterval. The rate of change of the slope of E is given by

$$\dot{E}' = -VE'' - V'E', \tag{B4}$$

so that the uniformity of E in the subinterval implies that

$$\dot{E}' = 0 \,\forall\, \mu_- < \mu < \mu_+, \tag{B5}$$

indicating that *a subinterval in which E is uniform can only change at its boundaries while at all interim points the value of E is conserved*. For consistency, it can be shown that this extremum principle for a subinterval degenerates to the extremum principle at a point in the limit $\mu_+ - \mu_- \to 0$.

This principle can be extended to the two-dimensional inviscid free shallow-water equations where it dominates the potential vorticity dynamics.

REFERENCES

Adam, O., and N. Paldor, 2009: Global circulation in an axially symmetric shallow water model forced by equinoctial differential heating. *J. Atmos. Sci.,* **66,** 1418–1433.

Dickinson, R. E., 1971: Analytical model for zonal winds in the tropics. I. Details of the model and gross features of the zonal mean troposphere. *Mon. Wea. Rev.,* **99,** 501–510.

Dima, I. M., and J. M. Wallace, 2003: On the seasonality of the Hadley cell. *J. Atmos. Sci.,* **60,** 1522–1527.

Esler, J. G., L. M. Polvani, and R. A. Plumb, 2000: The effect of the Hadley circulation on the propagation and reflection of planetary waves in a simple one-layer model. *J. Atmos. Sci.,* **57,** 1536–1556.

Fang, M., and K. K. Tung, 1996: A simple model of nonlinear Hadley circulation with an ITCZ: Analytic and numerical solutions. *J. Atmos. Sci.,* **53,** 1241–1261.

——, and ——, 1997: The dependence of the Hadley circulation on the thermal relaxation time. *J. Atmos. Sci.,* **54,** 1379–1384.

——, and ——, 1999: Time-dependent nonlinear Hadley circulation. *J. Atmos. Sci.,* **56,** 1797–1807.

Held, I. M., and A. Y. Hou, 1980: Nonlinear axially symmetric circulations in a nearly inviscid atmosphere. *J. Atmos. Sci.,* **37,** 515–533.

Hou, A. Y., 1984: Axisymmetric circulations forced by heat and momentum sources: A simple model applicable to the Venus atmosphere. *J. Atmos. Sci.,* **41,** 3437–3455.

——, and R. S. Lindzen, 1992: The influence of concentrated heating on the Hadley circulation. *J. Atmos. Sci.,* **49,** 1233–1241.

Lee, S., 1999: Why are the climatological zonal winds easterly in the equatorial upper troposphere? *J. Atmos. Sci.,* **56,** 1353–1363.

Lindzen, R. S., and A. Y. Hou, 1988: Hadley circulations for zonally averaged heating centered off the equator. *J. Atmos. Sci.,* **45,** 2416–2427.

Plumb, R. A., and A. Y. Hou, 1992: The response of a zonally symmetric atmosphere to subtropical thermal forcing: Threshold behavior. *J. Atmos. Sci.,* **49,** 1790–1799.

Polvani, L. M., and A. H. Sobel, 2002: The Hadley circulation and the weak temperature gradient approximation. *J. Atmos. Sci.,* **59,** 1744–1752.

Schneider, E. K., 1977: Axially symmetric steady-state models of the basic state for instability and climate studies. Part II. Nonlinear calculations. *J. Atmos. Sci.,* **34,** 280–296.

——, 1987: A simplified model of the modified Hadley circulation. *J. Atmos. Sci.,* **44,** 3311–3328.

——, and R. S. Lindzen, 1977: Axially symmetric steady-state models of the basic state for instability and climate studies. Part I. Linearized calculations. *J. Atmos. Sci.,* **34,** 263–279.

Schneider, T., 2006: The general circulation of the atmosphere. *Annu. Rev. Earth Planet. Sci.,* **34,** 655–688.

Shell, K. M., and I. M. Held, 2004: Abrupt transition to strong superrotation in an axisymmetric model of the upper troposphere. *J. Atmos. Sci.,* **61,** 2928–2935.

Vallis, G. K., 2006: *Atmospheric and Oceanic Fluid Dynamics.* Cambridge University Press, 745 pp.

Walker, C. C., and T. Schneider, 2005: Response of idealized Hadley circulations to seasonally varying heating. *Geophys. Res. Lett.,* **32,** L06813, doi:10.1029/2004GL022304.

——, and ——, 2006: Eddy influences on Hadley circulations: Simulations with an idealized GCM. *J. Atmos. Sci.,* **63,** 3333–3350.